Low, G. M. Rosair, F. Teixidor, C. Viñas, A. J. Welch, A. S. Weller, *Contemporary Boron Chemistry* (Eds.: M. G. Davidson, A. K. Hughes, T. B. Marder, K. Wade), Royal Society of Chemistry, Cambridge, **2000**, p. 329.

[2] a) D. R. Baghurst, R. C. B. Copley, H. Fleischer, D. M. P. Mingos, G. O. Kyd, L. J. Yellowlees, A. J. Welch, T. R. Spalding, D. O'Connell, *J. Organomet. Chem.* **1993**, *447*, C14; b) A. J. Welch, A. S. Weller, *J. Chem. Soc. Dalton Trans.* **1997**, 1205.

[3] a) S. Dunn, G. M. Rosair, R. L. Thomas, A. S. Weller, A. J. Welch, *Angew. Chem.* **1997**, *109*, 617; *Angew. Chem. Int. Ed. Engl.* **1997**, *36*, 645; b) S. Dunn, G. M. Rosair, A. S. Weller, A. J. Welch, *Chem. Commun.* **1998**, 1065; c) S. Dunn, R. M. Garrioch, G. M. Rosair, L. Smith, A. J. Welch, *Collect. Czech. Chem. Commun.* **1999**, *64*, 1013.

[4] R. M. Garrioch, P. Kuballa, K. S. Low, G. M. Rosair, A. J. Welch, *J. Organomet. Chem.* **1999**, *585*, 57.

[5] For both structure determinations: Crystals grown by diffusion of a $CH_2Cl_2$:40/60 petroleum ether (1:5) solution at 263 K, Bruker *P*4 diffractometer, 160(1) K, $Mo_{K\alpha}$ radiation, $\lambda = 0.71073$ Å, $2\theta_{max} = 50^\circ$, corrections for absorption effects ($\Psi$-scans), Lorentz and polarisation effects, structure solved by direct methods and refined (against $F^2$) by full-matrix least-squares methods. Crystal data for **1**: $C_{22}H_{30}B_9Rh$, $M_r = 494.66$: crystal size $0.15 \times 0.32 \times 0.22$ mm, triclinic, $P\bar{1}$, $a = 9.7270(14)$, $b = 10.7460(12)$, $c = 12.1641(17)$ Å, $\alpha = 106.834(9)$, $\beta = 105.519(10)$, $\gamma = 98.800(9)^\circ$, $V = 1135.4(3)$ Å$^3$, $Z = 2$, $\rho_{calcd} = 1.447$ g cm$^{-3}$, $F(000) = 504$, $\mu = 0.761$ mm$^{-1}$, of 3896 unique reflections 3289 were observed [$F_o > 4\sigma(F_o)$], 308 parameters, $R_1 = 0.0385$, $wR_2 = 0.0824$ (for observed data), $S = 1.033$, max. and min. residual electron density: 0.398 and $-0.557$ e Å$^{-3}$. Crystallographic data (excluding structure factors) for the structures reported in this paper have been deposited with the Cambridge Crystallographic Data Centre as supplementary publication no. CCDC-149160 (**1**) and -149161 (**2**). Copies of the data can be obtained free of charge on application to CCDC, 12 Union Road, Cambridge CB21EZ, UK (fax: (+44) 1223-336-033; e-mail: deposit@ccdc.cam.ac.uk).

[6] J. C. Jeffery, F. G. A. Stone, I. Topaloğlu, *Polyhedron* **1993**, *12*, 319.

[7] Crystal data for **2**: $(C_{14}H_{20}B_9ORh)_4 \cdot \mathbf{1} \cdot x\,CH_2Cl_2 \cdot C_5H_{12}$, $M_r =$ 1811.10*, crystal size $0.55 \times 0.52 \times 0.24$ mm, monoclinic, *C*2/*c*, $a = 20.830(5)$, $b = 28.683(8)$, $c = 15.916(3)$ Å, $\beta = 106.84(2)^\circ$, $V = 9101(4)$ Å$^3$, $Z = 4$, $\rho_{calcd} = 1.322$* g cm$^{-3}$, $F(000) = 3640$*, $\mu = 0.813$* mm$^{-1}$, of 7849 unique reflections 4003 were observed [$F_o > 4\sigma(F_o)$], 541 parameters, $R_1 = 0.0973$, $wR_2 = 0.2140$ (for observed data), $S = 0.984$, max. and min. residual electron density: 1.188 and $-2.667$ e Å$^{-3}$. See ref. [5]. (*$M_r$, $\varrho_{calcd}$, $F(000)$ and $\mu$ calculated on the basis of modeling the fractional $CH_2Cl_2$ solvate as an approximate triangle of 50% occupancy carbon atoms in general space).

[8] mass spectrometry: $CH_2Cl_2$ solution diluted with $CH_3OH$ and $N(CH_2CH_2OH)_3$, Thermoquest LCQ ion trap mass spectrometer, negative ion MS, mass range *m*/*z* 100–2000. MS/MS product ion spectra were obtained using a precursor ion mass window of 14 amu and collision energy between 24% and 30% of maximum. Molecular ion range *m*/*z* 1611–1623, centered on *m*/*z* 1616. Successive product-ion MS/MS scans, starting from *m*/*z* 1616, showed consecutive losses of $2 \times$ OH.

[9] Stirring of a THF solution of **1** overnight with excess NaOH under $N_2$ affords compound **2** in ca. 40% yield (not yet optimised). Full details will be reported later.

[10] a) The compound $[\{Ru(Et_2C_2B_4H_4)Co(Et_2C_2B_3H_3Bu)\}_4]$ is tetrameric with cobaltacarborane sandwiches linked by exopolyhedral Ru atoms. K. G. Parker, J. M. Russell, M. Sabat, R. N. Grimes, *Collect. Czech. Chem. Commun.* **1999**, *64*, 819; b) The compound $[\{Hg(C_2B_{10}H_{10})\}_4]$ is tetrameric and icosahedral but is not a metallacarborane in the sense that the metal atom is not part of the heteroborane cage. X. Yang, C. B. Knobler, M. F. Hawthorne, *Angew. Chem.* **1991**, *103*, 1519; *Angew. Chem. Int. Ed. Engl.* **1991**, *30*, 1507.

[11] M. F. Hawthorne, D. C. Young, P. A. Wegner, *J. Am. Chem. Soc.* **1965**, *87*, 1818.

[12] P. T. Greene, R. F. Bryan, *Inorg. Chem.* **1970**, *9*, 1464.

[13] H. C. Kang, Y. K. Do, C. B. Knobler, M. F. Hawthorne, *Inorg. Chem.* **1988**, *27*, 1716.

[14] A. E. Skaugset, T. B. Rauchfuss, S. R. Wilson, *Organometallics* **1990**, *9*, 2875.

# Structure and Dynamics of the Host–Guest Complex of a Molecular Tweezer: Coupling Synthesis, Solid-State NMR, and Quantum-Chemical Calculations**

Steven P. Brown, Torsten Schaller, Uta P. Seelbach, Felix Koziol, Christian Ochsenfeld, Frank-Gerrit Klärner, and Hans Wolfgang Spiess*

Supramolecular chemistry and noncovalent interactions are of major importance in many biological systems, for example in enzyme–substrate binding or antigen–antibody recognition, as well as in the design of new materials by molecular self-assembly.[1] An example is receptor **1**, which belongs to a family of molecules termed "molecular tweezers", due to their concave–convex topology and their propensity to selectively form complexes with electron-deficient aromatic and aliphatic compounds as well as with organic cations.[2] This high selectivity has been correlated with a markedly negative electrostatic potential, by using semiempirical and quantum-chemical calculations, for the concave side of the molecular tweezer.[3]

Hunter and Packer described a supramolecular structure determination, based on the empirical calculation of complexation-induced $^1$H NMR shifts in solution[4] employing the empirical methods[5] developed for the prediction of $^1$H NMR shifts of proteins. As further illustrated by, for example, the study of the dimerization of formic acid in a matrix at 7 to 40 K using IR spectroscopy,[6] a quantitative elucidation of the structure, dynamics, and electronic properties of such complex systems requires the coupling of advanced techniques of physical characterization and theoretical chemistry. The results of such an endeavour, which we describe here, can then provide guidelines for generating new structures.

Central to our approach are advances in high-resolution $^1$H solid-state NMR based on fast magic-angle spinning (MAS).[7] At rotation frequencies above 30 kHz, sufficient line narrowing is achieved such that $^1$H resonances due to chemically distinct protons can be distinguished.[8] Moreover, fast MAS can be combined with double-quantum (DQ) spectroscopy[9]

[*] Prof. Dr. H. W. Spiess, Dr. S. P. Brown
Max-Planck-Institut für Polymerforschung
Postfach 3148, 55021 Mainz (Germany)
Fax: (+49) 6131-379320
E-mail: spiess@mpip-mainz.mpg.de

Dr. T. Schaller, U. P. Seelbach, Prof. Dr. F.-G. Klärner
Institut für Organische Chemie der Universität Essen
45117 Essen (Germany)

F. Koziol, Dr. C. Ochsenfeld
Institut für Physikalische Chemie, Universität Mainz
55099 Mainz (Germany)

[**] S.P.B. thanks the Alexander von Humboldt Foundation for a research fellowship. C.O. acknowledges financial support by a Liebig "Habilitation" fellowship from the Fonds der Chemischen Industrie (FCI). This work was supported by the Deutsche Forschungsgemeinschaft (SFB 452) and the FCI. We thank Dr. Ingo Schnell for his involvement in the early part of this project, Dr. Kay Saalwächter for advice concerning the heteronuclear experiment, and Dr. Ulrich Burkert for his help during the synthesis of the complex.

Supporting information for this article is available on the WWW under http://www.angewandte.com or from the author.

to provide access to structural and dynamic information exploiting site-resolved dipolar couplings. This yields specific proton–proton proximity information and allows complex dynamic processes to be quantified. In particular, key elements of supramolecular organization, namely hydrogen bonds and $\pi-\pi$ interactions can be clearly unravelled.[8] Furthermore, the $^1$H chemical shifts resulting from supramolecular organization can be assigned quantitatively to specific molecular packing arrangements by means of quantum-chemical calculations.[10]

To date, molecular tweezer host–guest complexes have been investigated by $^1$H solution-state NMR exploiting the large upfield shifts of the substrate resonances, caused by the ring currents due to the aromatic host, upon complexation. For the specific complex studied here, complex formation and dissociation in $CDCl_3$ at room temperature between the napthalene-spaced tweezer **1** and 1,4-dicyanobenzene **2** is fast with respect to the NMR timescale, as evidenced

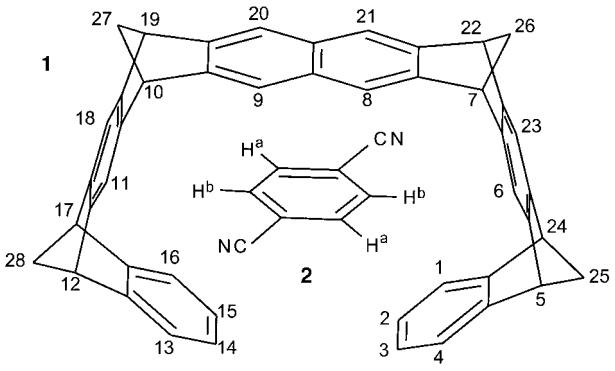


by a single-guest $^1$H resonance shifted by 4.35 ppm relative to that observed for **2** alone. A solid-state investigation has the advantage that the guest remains complexed on the timescale of the NMR experiment and, thus, the structure and dynamics of the host–guest complex can be probed directly. An X-ray single-crystal structure is available for **1@2**;[2b] therefore, this study offers the opportunity to check the reliability of our approach and to demonstrate that additional complementary insight can be provided.

Figure 1 a presents a rotor-synchronized $^1$H (700 MHz) DQ MAS NMR spectrum of **1@2**. In a $^1$H DQ MAS experiment, the evolution of a DQ coherence due to a pair of dipolar-coupled protons is correlated with that of the single-quantum (SQ) coherences of the two individual protons, to allow an unambiguous assignment of pairs of like and unlike protons.[8] The $^1$H solid-state NMR peak assignment (Table 1) follows from a $^1$H–$^{13}$C heteronuclear correlation[11] spectrum of **1@2** (Figure 1 b), recorded using a recently developed recoupled polarization-transfer (REPT) experiment,[12] which employs rotational-echo double-resonance (REDOR) recoupling.[13] Significant differences between the solid- and solution-state $^1$H chemical shifts are observed: In particular, the guest protons, which are equivalent in solution, differ in the solid state ($\Delta\delta = 3.6$). This splitting is a strong indication of ring-current effects,[8b, 14] as discussed below.

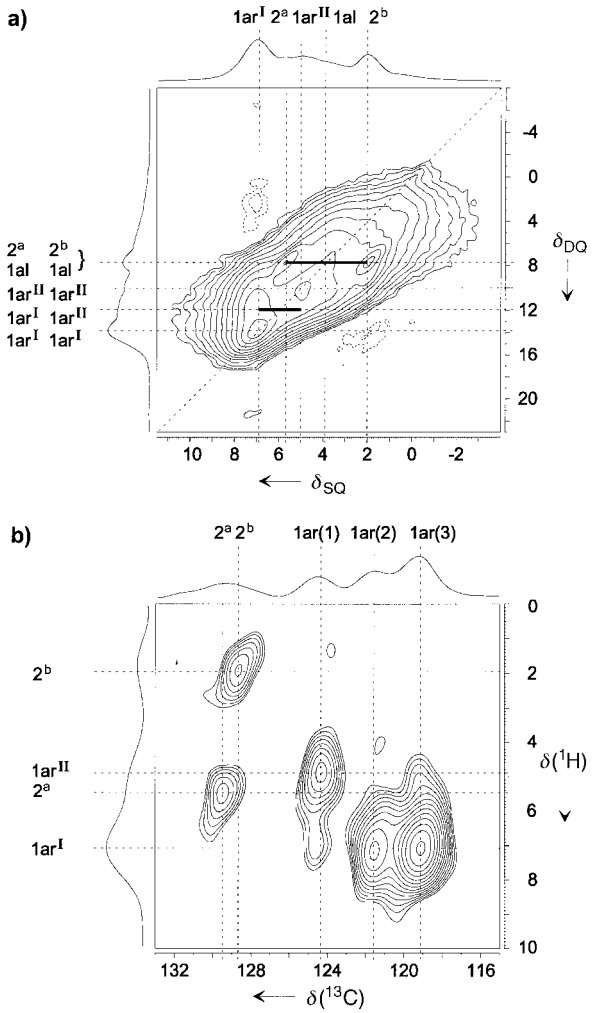


Figure 1. a) Rotor-synchronized $^1$H(700.1 MHz) DQ MAS NMR spectrum, together with skyline projections, of **1@2**, recorded under MAS at 30 kHz using one cycle of the BABA recoupling sequence for the excitation and reconversion of DQCs. b) The aromatic region of a $^1$H (700.1 MHz)–$^{13}$C REPT-HSQC NMR correlation spectrum, together with sum projections, of **1@2**, recorded under MAS at 30 kHz. The recoupling time equaled one rotor period, such that predominantly only one-bond correlations are selected. The sample temperature equalled 321 K in both cases. The notation 1 ar and 1 al refers to host aromatic and alkyl protons, respectively, while $2^a$ and $2^b$ refer to the two distinct guest aromatic protons.

Table 1. Experimental and ab initio $^1$H chemical shifts for **1@2**.

| | Solution-state NMR | Solid-state NMR | Ab initio (monomer) | Ab initio (dimer) |
|---|---|---|---|---|
| $H^a$ (guest) | 3.5 | 5.6 | 5.5 | 5.2 |
| $H^b$ (guest) | 3.5 | 2.0 | 2.5 | 2.1 |
| H2,3,14,15 | 6.4 | 4.9 | 6.6 | 5.5–5.6 |
| $H_{arom}$ (host) | 7.0–7.2 | 7.1–7.2 | 7.2–8.0 | 6.9–7.7 |
| $H_{bridgehead}$ | 4.1 | 3.8[a] | 3.9–4.2 | 3.3–4.0 |
| H25,28[b] | 2.4 | 2.0–3.8[a] | 2.2 | 2.1 |
| H26,27[b] | 2.5 | 0.6–2.3[a] | 2.0–2.1 | 0.4–1.0 |

[a] These $^1$H chemical shifts were determined from the alkyl region of the $^1$H–$^{13}$C correlation spectrum (not shown). [b] Note that the two protons in each $CH_2$ group are inequivalent.

We further performed quantum-chemical calculations to determine the structure and NMR chemical shifts of **1@2**. For the structure determination, we employed newly developed

  1433-7851/01/4004-0718 $ 17.50+.50/0 *Angew. Chem. Int. Ed.* **2001**, *40*, No. 4

linear-scaling methods,[15] at the Hartree–Fock (HF) level. NMR chemical shifts were calculated using the GIAO method (gauge including atomic orbitals)[16] at the HF level. In this way, we calculate the electronic structure and chemical shifts explicitly, which differs from the (empirical) approach of calculating ring currents.[17] Table 1 also presents $^1$H chemical shifts obtained by the quantum-chemical calculations for a single **1@2** complex and a pair of **1@2** complexes in the arrangement shown in Figure 2a (denoted as monomer and dimer, respectively). The good agreement between the monomer calculation and the experimental solid-state guest $^1$H chemical shifts reveals that these values are largely determined by *intracomplex* effects. We also note that the average deviation in guest-to-host aromatic carbon–carbon distances is less than 5% when comparing the ab initio monomer and X-ray structures. In contrast, the marked difference between the solid- and solution-state $^1$H chemical shifts of host aromatic protons (H2,3,14,15) on the "tweezer tip" can only be explained by considering a dimer. *Intercomplex* effects are apparent from Figure 2a, which shows that these pairs of aromatic protons are directed towards the naphthalene unit of the next host. Additional effects of neighbouring monomer units are expected to only be important for the most exposed protons of the tweezer, namely, the $CH_2$ groups.

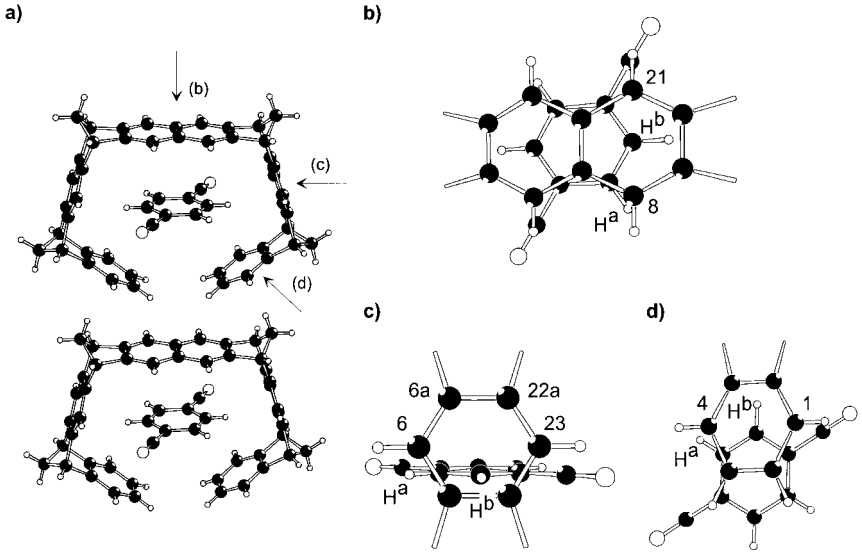


Figure 2. The solid-state packing arrangement of **1@2**, as determined by an X-ray single-crystal investigation.[2b] Large white, large black, and small white circles represent nitrogen, carbon, and hydrogen atoms, respectively. In b)–d), views through the naphthalene unit (b), and inner (c) and outer (d) benzene rings, respectively, are shown. The distance from $H^b$ to the center of the inner benzene ring is 260 pm, as opposed to 404 pm to the middle of the naphthalene unit and 314 pm to the center of the outer benzene ring (distances are given for the ab initio structure). Specific carbon and hydrogen atoms are labeled according to the above chemical structure; the notation *x*a refers to the quaternary carbon between carbons $x$ and $x+1$.

Quantum-chemical calculations are able to elucidate the role of different chemical units within a molecule. Therefore, we also calculated the $^1$H chemical shifts of the guest protons due to the three host aromatic moieties, namely the central napthalene unit, and the inner and outer benzene rings (Figure 2b–d). These results will be discussed in detail elsewhere but we note the main conclusions here. Firstly, the guest $^1$H chemical shifts, derived by summing the changes due to the separate aromatic moieties, are in good agreement with the values calculated for the whole system. It can thus be concluded that the only influence of the linking norbornadiene units is to determine the positioning of the host aromatic moieties. Secondly, the difference between the guest $^1$H chemical shifts is mainly due to the arrangement of the guest with respect to the inner benzene ring (Figure 2c). Thus, our combined experimental and theoretical approach is able to identify specific intermolecular interactions, which will be particularly useful for the structural elucidation of systems, for which X-ray single crystal structures are not available.

A unique strength of solid-state NMR is its ability to probe molecular dynamics with site selectivity.[18] Figure 3 presents slices taken from $^1$H DQ MAS spectra (each slice at $\delta_{DQ} = 7.6$) recorded at different temperatures. The peaks due to the guest protons $H^a$ ($\delta = 5.6$) and $H^b$ ($\delta = 2.0$) disappear upon heating, to indicate dynamic processes (see Figure 3), in which the two types of guest protons are exchanged by either a) a 180° flip about the long axis of the guest or b) a 60° rotation between two equivalent sites in the complex. A quantitative analysis is hampered by the peak at $\delta = 3.9$ due to host alkyl protons—the fast exchange peak would be expected to appear at exactly this position. We note, though, that no peak was observed in a slice corresponding to the guest $^{13}$C CH resonance in a $^1$H–$^{13}$C correlation spectrum recorded at 410 K (spectrum not shown). Thus, we conclude that, at this temperature, the exchange process is in the intermediate regime, namely coalescence. From the difference in the chemical shifts of the guest protons $H^a$ and $H^b$ ($\Delta\delta = 3.6$), the rate constant for the exchange process at 410 K can be estimated to be 5600 $s^{-1}$ corresponding to a Gibbs free enthalpy of activation $\Delta G^{\ddagger}$ of 72 kJ mol$^{-1}$.[19]

To conclude, for the host–guest complex **1@2**, a combined experimental and theoretical approach provides structural information, namely the importance of both intra- and intercomplex interactions as well as the role of the separate aromatic moieties, whereas temperature-dependent solid-state NMR spectra probe the guest dynamics. All experiments were performed on only 10 mg of a powdered sample, without isotopic labeling. Therefore, it is envisaged that solid-state NMR combined with quantum chemistry can become as valuable to the chemist as solution-state NMR is today. The approach described here exploits the sensitivity of $^1$H chemical shifts to aromatic ring currents and can be applied to both crystalline and amorphous systems alike. As these effects occur over quite a long range (more than 700 pm),[10b] we expect such effects to be of general importance in all aromatic systems. It is only now, however,

  1433-7851/01/4004-0719 $ 17.50+.50/0 

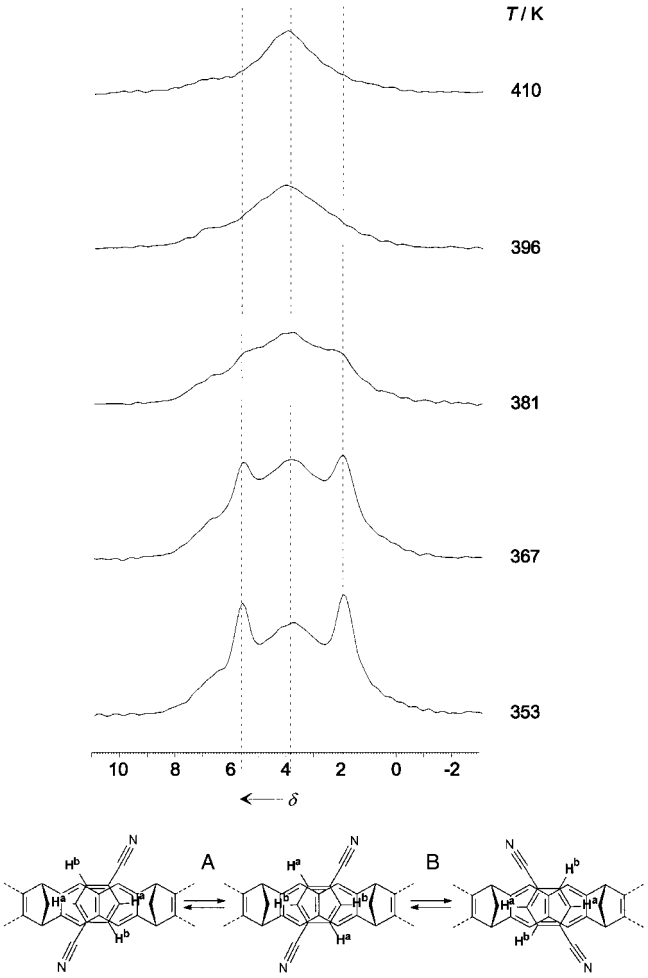


Figure 3. The effect of temperature $T$ on slices ($\delta_{DQ} = 7.6$) taken from $^1$H (700.1 MHz) DQ MAS NMR spectra of **1@2**. At the bottom, the dynamic processes consistent with the observed NMR results are shown. The two processes (A) and (B) cannot be distinguished by current experiments.

that solid-state NMR and quantum chemistry have developed sufficiently to allow the routine experimental observation of the $^1$H chemical shifts and the quantitative analysis of intermolecular ring-current effects in relatively large systems, respectively.

## *Experimental Section*

The synthesis of **1** is described in ref. [2b]. The complex with **2** is formed by dissolving the host and guest in a 1:1 molar ratio mixture of methanol/dichloromethane (1/1), followed by evaporation of the solvent at room temperature to yield colorless crystals.

Solid-state NMR experiments were performed on a Bruker DRX700 narrow-bore spectrometer operating at $^1$H and $^{13}$C Larmor frequencies of 700.1 and 176.1 MHz, respectively, with a double-resonance 2.5 mm MAS probe, 90° pulse lengths of 2.0 μs on both channels, and a recycle delay of 1 s. In all spectra, the increment in $t_1$ was set equal to one rotor period. For the DQ MAS [REPT-HSQC] experiment, for each of the 64 [24] increments, 16 [1024] transients were averaged. In the contour plots (Figure 1a, b), solid and dashed lines represent positive and negative contours, respectively; the bottom contour corresponds to 2.0 and 8.0 % of the maximum intensity (in Figure 2a, b) and subsequent contours corresponding to a multiplicative increment of 1.4 and 1.2.

Quantum-chemical calculations[10] were performed with the packages Q-Chem and TURBOMOLE.[20] The structure of **1@2** was optimized at the Hartree–Fock (HF) level employing a 6-31G* basis.[21] $^1$H chemical shifts were calculated using the GIAO method at the HF level, and are given relative to tetramethylsilane (TMS). For the monomer calculation, a (triple-ζ polarization (TZP) basis was used.[22] The dimer was constructed by arranging two **1@2** complexes (with the optimized quantum-chemical structure) at a separation given by the single-crystal structure.[2b] Dimer correction values were obtained as the difference between the dimer and monomer $^1$H chemical shifts at the GIAO-HF/SVP[22] level; these values were added to the monomer values calculated at the GIAO-HF/TZP level. The dimer $^1$H chemical shifts are given in Table 1. The $^1$H absolute shieldings for TMS (calculated at HF/6-31*) are $\delta = 32.4$ (GIAO-HF/TZP) and 32.3 (GIAO-HF/SVP).

The solution-state NMR assignments, as well as additional details concerning the experimental solid-state NMR and quantum-chemical calculations, are provided as Supporting Information.

Received: July 24, 2000 [Z15507]


[1] *Comprehensive Supramolecular Chemistry* (Eds.: J. L. Atwood, J. E. D. Davies, D. D. MacNicol, F. Vögtle, K. S. Suslick), Elsevier, Oxford, **1996**.

[2] a) F.-G. Klärner, J. Benkhoff, R. Boese, U. Burkert, M. Kamieth, U. Naatz, *Angew. Chem.* **1996**, *108*, 1195; *Angew. Chem. Int. Ed. Engl.* **1996**, *35*, 1130; b) F.-G. Klärner, U. Burkert, M. Kamieth, R. Boese, J. Benet-Buchholz, *Chem. Eur. J.* **1999**, *5*, 1700.

[3] a) M. Kamieth, F.-G. Klärner, F. Diederich, *Angew. Chem.* **1998**, *110*, 3497; *Angew. Chem. Int. Ed. Engl.* **1998**, *37*, 3303; b) F.-G. Klärner, J. Panitzky, D. Preda, L. T. Scott, *J. Mol. Model.* **2000**, *6*, 318.

[4] C. A. Hunter, M. J. Packer, *Chem. Eur. J.* **1999**, *5*, 1891.

[5] L. Szilagyi, *Prog. Nucl. Magn. Reson. Spectrosc.* **1995**, *27*, 325.

[6] M. Gantenberg, M. Halupka, W. Sander, *Chem. Eur. J.* **2000**, *6*, 1865.

[7] a) S. F. Dec, C. E. Bronninmann, R. A. Wind, G. E. Maciel, *J. Magn. Reson.* **1989**, *82*, 454; b) H. J. Jakobsen in E*ncyclopedia of Nuclear Magnetic Resonance*, *Vol. 1* (Eds.: D. M. Grant, R. K. Harris), Wiley, Chichester, **1996**, p. 398.

[8] a) I. Schnell, S. P. Brown, H. Y. Low, H. Ishida, H. W. Spiess, *J. Am. Chem. Soc.* **1998**, *120*, 11784; b) S. P. Brown, I. Schnell, J. D. Brand, K. Müllen, H. W. Spiess, *J. Am. Chem. Soc.* **1999**, *121*, 6712.

[9] a) R. R. Ernst, G. Bodenhausen, A. Wokaun, *Principles of Nuclear Magnetic Resonance in One and Two Dimensions*, Clarendon, Oxford, **1987**; b) A. Pines, D. J. Ruben, S. Vega, M. Mehring, *Phys. Rev. Lett.* **1976**, *36*, 110.

[10] a) C. Ochsenfeld, *Phys. Chem. Chem. Phys.* **2000**, *2*, 2153; b) C. Ochsenfeld, S. P. Brown, I. Schnell, J. Gauss, H. W. Spiess, *J. Am. Chem. Soc.* **2001**, in press.

[11] a) B.-J. van Rossum, H. Förster, H. J. M. de Groot, *J. Magn. Reson.* **1996**, *124*, 516; b) A. Lesage, D. Sakellariou, S. Steuernagel, L. Emsley, *J. Am. Chem. Soc.* **1998**, *120*, 13194.

[12] K. Saalwächter, R. Graf, H. W. Spiess, *J. Magn. Reson.* **1999**, *140*, 471.

[13] T. Gullion, J. Schaefer, *J. Magn. Reson.* **1989**, *81*, 196.

[14] a) B.-J. van Rossum, G. J. Boender, F. M. Mulder, J. Raap, T. S. Balaban, A. Holzwarth, K. Schaffner, S. Prytulla, H. Oschkinat, H. J. M. de Groot, *Spectrochim. Acta A* **1998**, *54*, 1167; b) B.-J. van Rossum, PhD thesis, University of Leiden, **2000**.

[15] C. Ochsenfeld, *Chem. Phys. Lett.* **2000**, *327*, 216, and references therein.

[16] J. Gauss, *Ber. Bunsen-Ges. Phys. Chem.* **1995**, *99*, 1001, and references therein.

[17] P. Lazzeretti, *Prog. NMR Spectrosc.* **2000**, *36*, 1, and references therein.

[18] K. Schmidt-Rohr, H. W. Spiess, *Multidimensional Solid-State NMR and Polymers*, Academic Press, New York, **1994**.

[19] H. Günther, *NMR-Spektroskopie*, Thieme, Stuttgart, **1992**, p. 310 (Equations 9.11 und 9.12).

[20] a) *Q-Chem* (development version): Q-Chem Inc., Pittsburgh, PA, **1998**; b) R. Ahlrichs, M. Bär, M. Häser, H. Horn, C. Kölmel, *Chem. Phys. Lett.* **1989**, *162*, 165.

[21] W. J. Hehre, R. Ditchfield, J. A. Pople, *J. Chem. Phys.* **1972**, *56*, 2257.

[22] A. Schäfer, H. Horn, R. Ahlrichs, *J. Chem. Phys.* **1992**, *97*, 2571.


  1433-7851/01/4004-0720 $ 17.50+.50/0 